Electron-hole liquid and exciton and biexciton gas in elastically deformed silicon crystals

V. D. Kulakovskiĭ, V. B. Timofeev, and V. M. Édel'shteĭn

Institute of Solid State Physics, USSR Academy of Sciences
(Submitted 10 August 1977)
Zh. Eksp. Teor. Fiz. **74**, 372–383 (January 1978)

Exciton condensation into an electron-hole liquid (EHL) is investigated in silicon elastically deformed along the crystallographic directions [100], [110], and [111]. Analysis of the form of the recombination radiation (RR) spectrum is used to determine the binding energy φ and the equilibrium density n_0 of the EHL for different deformation directions. It is shown that with decreasing multiplicity of the degeneracy of the valence band and of the number of valleys in the conduction bands, φ and n_0 decrease. It is established that in Si crystals deformed along [100], the partial pressures of the exciton gas and of the gas of biexcitons are commensurate along the gas–liquid equilibrium line. The RR spectrum of the biexcitons was measured. The probability of annihilation of the exciton is calculated, the shape of its radiative spectrum is analyzed, and its binding energy is estimated at 0.55 ± 0.15 meV.

PACS numbers: 71.35.+z, 71.45.Nt, 71.20.+c

1. INTRODUCTION

It is well known that in the indirect semiconductors Si and Ge uniaxial elastic deformations lift the degeneracies in the bands. As a result, the average kinetic energy per pair of particles in the electron-hole liquid (EHL) increases, and the binding energy and the equilibrium density of the electron hole (e–h) pairs in the condensed phase decrease. The change of the EHD binding energy is accompanied by a substantial change of the partial composition of the saturated gas vapor along the gas–liquid coexistence line. Despite the complex composition of the gas phase (excitons, biexcitons, e–h pairs, etc.), all that has been observed up to now in the recombination radiation (RR) spectra were the exciton emission and low temperatures and the emission e–h pairs near the critical temperature.[1-2] The question of the experimental observation of the biexcitons in Si and Ge remained open. The reason lies in the fact that, owing to the low binding energy compared with the EHL, the biexciton gas turns out to be strongly dissociated even at exciton gas densities at which condensation into EHL takes place. The situation for biexciton observation becomes more favorable in uniaxially deformed crystals, in which the EHL binding energy is substantially decreased. In particular, in silicon deformed along [100] the partial pressures of the exciton and biexciton gases are of the same order along the gas–liquid equilibrium line.

We investigate in this paper the condensation into EHL in silicon elastically deformed along [100], [110], and [111], and have determined the binding energy φ and the equilibrium concentration n_0 in the EHL (Sec. 3). We study the kinetics of the EHL and exciton spectra (Sec. 4). The RR of the biexciton is observed under pulsed and stationary excitation (Sec. 5). The probability of the radiative decay of the biexciton is calculated (Sec. 6) and the form of the emission spectrum of the biexciton is approximated (Sec. 7).[1]

2. EXPERIMENTAL PROCEDURE AND CRYSTALS

We used single crystals of pure silicon with a concentration of the residual electrically active impurities (mainly boron) $n < 3 \times 10^{12}$ cm^{-3}. The samples were rectangular parallelepipeds with linear dimensions $1 \times 3 \times 7$ mm. The deformation was carried out along the largest linear dimension of the samples. Before each mounting in the cryostat, the samples were etched in a mixture of fluoric and nitric acids (1:3). The work was performed with the samples placed either in liquid helium or in its vapor, in the latter case to measure the RR at higher temperatures. At $T > 5$ K the temperature was stablized within 0.1 K.

Elastically deformed samples were placed between parallel planes of two plungers (~10 mm diam) of stainless steel liners of lead-tin alloy, 1.5 mm thick, were placed between the crystal and the plunger. A small pressure was first applied at room temperature, in which case the sample sank slightly into the liners. This was followed by cooling to helium temperature. It was then possible to deform the samples to a pressure on the order of 7 kbar. Under the conditions of our experiments the homogeneity of the deformation was high enough, judging from the free-exciton emission line shape. Thus, at a spectral resolution 0.25 meV and under volume excitation we observed no inhomogeneous broadening of the exciton line up to uniaxial pressures of 7 kbar.

The nonequilibrium carriers were excited either by continuous or by pulsed sources. Pulsed pumping was with a copper-vapor laser (power and duration of a single pulse were 3 kW and 10 nsec, the pulse repetition frequency was 15 kHz, and the lasing wavelength was 5105 A). The laser could produce pulsed excitation of e–h pairs near the surface of the sample, with a density ~5×10^{17} cm^{-3}. The source of the continuous volume excitation was an aluminum-yttrium garnet laser

(wavelength 1.064 μm, power 5 W). This source ensured a stationary concentration of the $e-h$ pairs up to ~10^{15} cm^{-3} at pressures ~6 kbar.

The radiation receiver was a photomultiplier with cathode S-1, cooled to $t = -60\,°C$ and operating in the photon-counting regime. In the case of excitation with the aid of a pulsed laser we used a registration system operating in the strobe-integration regime. The duration of the strobing pulse was varied in the range 0.1–10 μsec. When working with the constant source, its radiation was modulated with a chopper at a frequency 60 Hz and a pulse duration 0.2 msec. This quasi-continuous regime reduced sample heating to a minimum. In this case the registration was in the synchronous-detection regime.

The spectral instrument was a double monochromator with a dispersion 10 Å/mm in the working region.

3. RECOMBINATION SPECTRA OF ELECTRON-HOLE LIQUID IN SILICON ELASTICALLY DEFORMED ALONG [001], [011], AND [111]

In this section we are interested mainly in ascertaining how the restructuring of the energy spectrum, due to the lifting of the band degeneracy by the directional deformation, alters the binding energy and the equilibrium density of the carriers in the EHL. To this end we investigated the recombination-radiation spectra of silicon strongly deformed along the axes [100], [110], and [111] (i.e., Si (1–2), (1–4), and (1–6), where the first number denotes the multiplicity of the degeneracy of the valence band, and the second of the number of the lowest split-off electron valleys).

At pressures $p < p_{cr}$, a continuous restructuring of the EHL recombination spectrum takes place as the deformation is increased. Only starting with a pressure p_{cr}, when the splitting in the bands becomes comparable with the corresponding values of the Fermi energies of the electrons and holes in the EHL, does the RR spectrum of the EHL acquire the canonical form for each given compression direction and is independent of the applied pressure.[4,5] The pressures p_{cr} for the compression directions [100], [110], and [111] turned out to be 20, 30, and 40 kgf/mm^2, respectively.

Figure 1 shows the recombination spectra of Si (1–6), Si (1–4), and Si (1–2) obtained under conditions of strong uniaxial deformation 24, 42, and 48 kgf/mm^2, respectively). The spectra were measured at $T = 1.8$ K and under pulsed laser pumping at 30 kW/cm^2. For comparison the figure shows the spectrum of undeformed Si (2–6). Each of the presented spectra contains a wide band L corresponding to the EHL emission, and free-exciton emission lines FE, marked on the figure by arrows (the TO-LO structure corresponds to recombination processes with emission of TO and LO phonons). We call attention to the fact that in Si (1–2), besides the lines of the RR of the EHL and of the free excitons, there is also observed a biexciton RR line M. The RR of biexcitons is treated in Secs. 5–7. To separate the contour of the EHL RR spectrum from the RR spectral
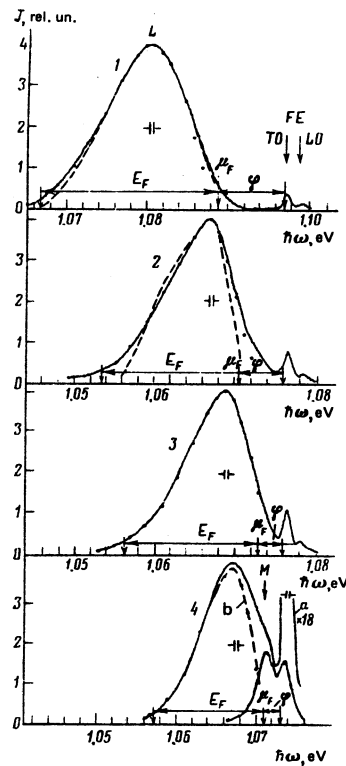

FIG. 1. RR spectra of undeformed Si (2–6) (1) and of silicon deformed along the axes [111] Si (1–6) (2), [110] Si (1–4) (3) and [100] Si (1–2) (4) under pulsed excitation (30 kW/cm^2, $T = 1.8$ K), recorded with a delay of 0.05 μsec relative to the excitation pulse. The spectrum a for Si (1–2) corresponds to a delay of 0.7 μsec, and curve b corresponds to the EHL RR contour obtained by subtracting the M line. The approximation of the spectra with the aid of expression (1) for Si (2–6) and Si (1–6) is shown dashed, while the points show the curves obtained using the two fit parameters n_0 and Γ_0.

dependence measured at a time delay $\tau_d = 0.05$ μsec relative to the excitation pulse, we subtracted the suitably normalized M line recorded at a delay $\tau_d = 0.45$ μsec. It is seen from Fig. 1 that as the degeneracy is lifted the width of the EHL band decreases, and its maximum and "violet" edge lies closer to the exciton line. In the deformed crystals there is a noticeable increase of the exciton radiation intensity relative to the EHL band, as well as an increase of the condensation threshold. These results already demonstrate qualitatively that the lifting of the degeneracy as a result of the splitting of the valence band and of the decrease of the "multivalley character" lowers the binding energy per pair of particles in the EHL and its equilibrium density.

The equilibrium concentration of the $e-h$ pairs in the EHL in Si and Ge is usually determined by analyzing the shape of the RR spectrum, using the expression[1-3,6,7]

$$J(h\nu) \sim \int_0^{h\nu} [\varepsilon(\varepsilon - h\nu)]^{1/2} \left[1 + \exp\left(\frac{\varepsilon - \varepsilon_F^{e'}}{kT}\right) \right]^{-1}$$

$$\times \left[1 + \exp\left(\frac{h\nu - \varepsilon - \varepsilon_F^{h'}}{kT}\right) \right]^{-1} d\varepsilon, \tag{1}$$

where $\epsilon_F^e(n_0)$ and $\epsilon_F^h(n_0)$ are the Fermi energies of the electrons and holes. The energy of the emitted photon is

$$\hbar\omega = h\nu + E_{gap} - \mathcal{E}_{xc} - \hbar\Omega, \tag{2}$$

where E_{gap} is the width of the forbidden band, $\mathcal{E}_{xc}$ is the sum of the exchange and correlation energies, and $\hbar\Omega$ is the energy of the emitted phonon. In this expression, no account is taken of the corrections that must be introduced into the state density $\rho(\epsilon)$ to allow for the

interactions between the particles. It follows from (1) that at a known temperature the sought density n_0 is given by a single fit parameter.

When the spectrum in Si is approximated with the aid of the distribution (1), it must also be recognized that the L band is a superposition of two broad bands with emission of the TO phonons (strong component) and LO phonons (weak component), separated in energy by $\hbar(\Omega^{TO} - \hbar\Omega^{LO}) = 1.8$ meV. The ratio of the intensities of the TO and LO components depends on the deformation direction. In Si (2-6) we have $J_{LO}/J_{TO} = 0.1$.[8] In deformed Si this ratio in the EHL was assumed equal to the measured ratio of the TO and LO components of the RR of the free excitons.

With the aid of (1) it is possible to describe satisfactorily the RR of the EHL in Si (2-6)[3,7] (Fig. 1, dashed) and in Si (1-2). In both cases the Fermi energies ϵ_F^e and ϵ_F^h of the electrons and holes are close to each other, and the integral in (1) is a convolution of two functions of equal width, so that the resultant contour $I(h\nu)$ is not sensitive to a small change of the state densities. In Si (1-4) and particularly in Si (1-6), for which $\epsilon_F^e/\epsilon_F^h \sim \frac{1}{4}$, the disparity between the calculated (dashed in Fig. 1) and experimental spectrum is substantial. Thus, the use of the density of states ρ in the form $\rho \sim \epsilon^{1/2}$, as in (1), is too rough an approximation and it is necessary to correct $\rho(\epsilon)$ for the interparticle interactions.

The corrections to ρ have a twofold character[9]: a) the $\epsilon(k)$ dependence is changed and the dispersion law ceases to be quadratic, and b) the energy levels of the excited states in the Fermi liquid, which are produced upon recombination of the $e-h$ pairs, the "holes" in the conduction band and the "electrons" in the valence band are broadened; the broadening increases with increasing distance from ϵ_F. An attempt can also be made to take the broadening into account by introducing an effective state density[10]

$$\rho_{eff}(\epsilon) = \frac{1}{\pi} \int d\epsilon_0 \, \rho(\epsilon_0) \Gamma(\epsilon_0) [\pi(\epsilon-\epsilon_0)^2 + \Gamma^2(\epsilon_0)]^{-1}. \tag{3}$$

The corrections to ρ both as a result of the change of the dispersion law and those due to the damping of the excited states lead to a smoother dependence of ρ_{eff} in comparison with $\epsilon^{1/2}$ near the bottom of the band. One can therefore hope that allowance for these corrections will make it possible to describe the "red tail" in the RR spectrum of the EHL. It is difficult to say beforehand which of these corrections predominates. From an investigation of the RR spectrum of the EHL in Ge in a magnetic field it follows that the broadening of the energy levels near the bottom of the band is large enough.[11]

In this paper we made an attempt to describe the RR spectrum by introducing into consideration only the damping of the excited states in the EHL. We used for ϵ_{eff} the expression (3), and chose $\Gamma(\epsilon)$ in the form[9]

$$\Gamma(\epsilon) = \Gamma_0(1-\epsilon/\epsilon_F)^2 \tag{4}$$

and assumed that $\Gamma_0^e/\Gamma_0^h = \epsilon_F^e/\epsilon_F^h$. The temperature was

TABLE I. Parameters of EHL in silicon.

	Si(2-6)	Si(1-6)	Si(1-4)	Si(1-2)	Si(1-2) calculation [12-13]
$n_0 \cdot 10^{-18}$, cm^{-1}	3.5 ± 0.05	0.98 ± 0.03	0.90 ± 0.03	0.48 ± 0.02	0.447
φ, MeV	8 ± 0.2	5.5 ± 0.2	3.1 ± 0.2	2 ± 0.2	1.88
$\epsilon_F^e \div \epsilon_F^h$, MeV	22.3	17	16.5	13.7	13.24
ϵ_F^h, MeV	14.4	13.6	12.3	9.3	9.06
Γ_0^h, MeV	2.2 ± 0.2	2.1 ± 0.2	2.0 ± 0.2	1.6 ± 0.2	

assumed equal to zero. Thus, two fit parameters were used, n_0 and Γ_0. The points on Fig. 1 show the obtained approximation curves for undeformed and deformed silicon. It is seen that they describe well the experimental spectra. The values of n_0 and Γ_0, and also of ϵ_F^e, ϵ_F^h, $E_F = \epsilon_F^e + \epsilon_F^h$ and φ are listed in Table I. The obtained values of Γ_0, as expected, increase with increasing ϵ_F. An estimate of Γ_0 by means of the formula $\Gamma_0 = \pi e^2 p_F^2/16\varkappa r_D \hbar^2$,[9] where e is the electron charge, $\varkappa$ is the permittivity, r_D is the screening, and p_F is the Fermi momentum, yields values that are approximately twice as large. The obtained values of n_0 and φ for Si (1-2) agree well with those calculated in.[12,13] We note also that the introduction of the parameter Γ_0 alters little the sought value of the equilibrium density (less than 10% for Si (2-6) and Si (1-2) and less than 20% for Si (1-6) and Si (1-4).

4. KINETICS OF RR SPECTRA IN SILICON

The lifetime of the nonequilibrium carriers in a drop in Si is determined by nonradiative processes. The most probable mechanism of $e-h$ drop annihilation is apparently Auger recombination. For this process, the lifetime in the EHL should be proportional to n^2. We can therefore expect the EHL lifetimes to be in a ratio

$$\tau_0 : \tau_{111} : \tau_{110} : \tau_{100} = 1 : 12 : 14 : 20,$$

where the subscript of τ denotes the deformation direction and τ_0 is the lifetime in the undeformed crystal.

It follows from the experiment (Figs. 2, 3) that the dependence of the RR of the EHL on the time can be described by an exponential only in Si (2-6), Si (1-6) and Si (1-4) at 1.8 K and in Si (2-6) at 4.2 K. A stronger dependence is observed in the remaining cases (particularly Si (1-2)). The lifetimes determined for Si (2-6), Si (1-6), and Si (1-4) at 1.8 K were
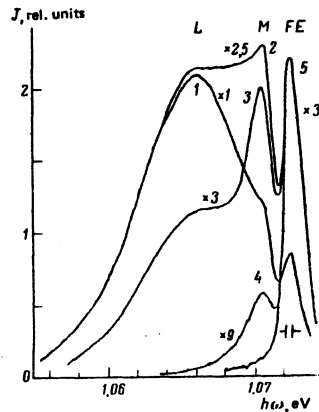

FIG. 2. Kinetics of the RR spectrum of Si (1-2) under pulsed excitation (30 kW/cm^2) and $T = 1.8$ K. Spectra 1-5 correspond respectively to delays of 0.05, 0.25, 0.35, 0.7, and 1.1 μsec relative to the exciting pulse. The points on Fig. 4 correspond to the M line measured under volume excitation.
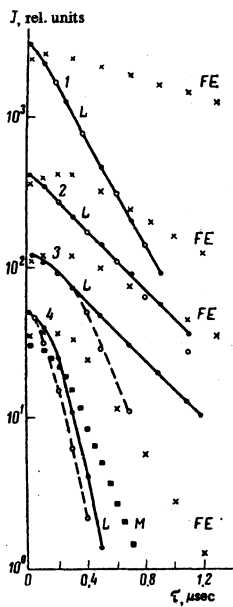
FIG. 3. Dependence of the emission line intensities of the excitons (FE), biexcitons (M), and EHL (L) on the delay relative to the excitation pulse (●—at $T = 2$ K, ○—at $T = 4.2$ K): 1—Si (2-6), 2—Si (1-6), 3—Si (1-4), 4—Si (1-2).

respectively 0.25, 0.45, and 0.5 μsec or $\tau_0 : \tau_{111} : \tau_{110}$ = 1:2:2, which deviates greatly from the expected values. Moreover, an estimate of τ_{100} from the experimental curve in the region $t = 0.2$-0.5 μsec yields a value $\tau_{100} < \tau_0$ ($\tau_{100} \sim 0.1$ μsec). It can thus be stated that in the considered case the annihilation of the electron hole drop (EHD) is not caused by Auger recombination of the e-h pairs in the EHL.

It is seen from the experimental $J_{ex}(t)$ dependence that the number of excitons still increases 0.1-0.2 μsec after the excitation pulse. This increase can be produced only by evaporation of the EHL and only in the case $n_T^* > n_{ex}$, with $n_T^* = n_T \exp(-2\alpha/n_0 R_{EHD} kT)$, where $n_T = g_{ex}(m_{ex} kT/2\pi\hbar^2)^{3/2} \exp(-\varphi/kT)$ is the thermodynamic equilibrium density of the exciton gas, g_{ex} and m_{ex} are respectively the statistical weight and the effective mass of the state density of the excitons, and α and R_{EHD} are the surface tension coefficient and the radius of the EHD. It was assumed in the estimates that $\alpha \sim \varphi n^{2/3}/9$[14] and the minimal $R_{EHD} \sim 10^{-6}$ cm. That the evaporation of the EHL is substantial, despite the large binding energies, is attested also by the discrepancies between $I_{EHD}(t)$ at $T = 2$ and 4.2 K even in Si (1-6) with $\varphi \sim 5$ meV.

To estimate n_{ex} we established a correspondence between the numbers of the excitons and the registered quanta per unit time in the case of weak stationary pumping ($n_{ex} = P\tau_{ex}/\hbar\omega$, where P is the absorbed power). The number of the registered quanta in the pulsed regime per unit of "net" time we found next that $\tau_d \lesssim 0.1$ μsec, $T = 2$ K, $n_{ex} \approx 10^{13}$-10^{14} in Si (2-6) and 10^{14}-10^{15} cm^{-3} in Si (1-2). (It was assumed in the calculation that the excited-region depth, which is determined by the diffusion of the excitons and by the spreading of the EHL after 0.1 μsec, is ~0.1 mm). The obtained values of n_{ex} exceed $n_T^*(2$ K) by several orders of magnitude ($n_T(2$ K) ~10^{10} and ~10^{12} in Si (2-6) and Si (1-2), respectively). It must therefore be assumed that the EHD temperature T_{EHD} is higher than the crystal temperature T_c. A large value of T_{EHD} compared with $T_{ex} \approx T_c$

was indicated also in [2] in an analysis of the shape of the RR curve of the EHL. According to calculations,[15] T_{EHD} can lie in the range $T_c < T_{EHD} < T_c(1 + v/s)$, where v is the EHD velocity and s is the speed of sound, with $v < s$, i.e., T_{EHD} can reach $2T_c$ at $v \sim s$. This temperature rise is sufficient to explain the experimentally observed n_{ex}. We note that the condensation process should have a cyclic character here. The EHD nucleus grows rapidly to dimensions corresponding to $n_{ex}(R_{EHD} < 3\tau v_T n_{ex}/n_0$,[16] where v_T is the thermal velocity of the excitons), heats up with little change in dimensions so long as $n_{ex} \gg n_T^*$, and evaporates rapidly when the reached value of T_{EHD} is such that $n_T^* > n_{ex}$. The produced gas cools down to T_c and is again condensed. The decrease of the RR intensity of the EHD is determined by the decrease of both R_{EHD} (with decreasing n_{ex}) and of the drop concentration. In this case it is incorrect to determine τ_{EHD} from the slope of $J_{EHD}(t)$ at $N_{EHD}^* = n - n_{ex} \lesssim 5n_{ex}$, even at a fixed excited volume. In deformed Si the ratio is $N_{EHD}^*/n_{ex} \lesssim 10$ even at $\tau_d = 0$, and furthermore the region occupied by the nonequilibrium gas increases with time. Thus, the values of τ_{EHD} obtained above do not reflect the lifetime of the EHD relative to the recombination of e-h pairs.

We measured the lifetime in the electron-hole plasma in Si doped with boron to 10^{17} cm^{-3} under pulsed excitation at a power 100 kW/cm^2. The excited volume is in this case much smaller, since the RR band in Si (1-2) at the instant of the excitation pulse is 1.5 times broader than the RR of an EHD in pure Si (1-2). The lifetimes obtained from the $J(t)$ curve for doped Si:B turned out to be large, particularly for Si (1-2): $\tau_0 = 0.3 \mu$sec, $\tau_{111} = 0.7\mu$sec and $\tau_{100} = 1\mu$sec.

In concluding this section we note that the strong decrease of the exciton lifetime in deformed crystals has not yet been fully explained. This decrease is observed already at pressures ~1 kgf/mm^2. With further increase of the deformation, up to 70 kgf/mm^2, τ_{ex} remains independent of p.

5. EMISSION OF BIEXCITONS IN UNIAXIALLY DEFORMED SILICON

When Si is deformed along [100], the maximum lifting of degeneracy takes place in the bands, and the binding energy in the EHL undergoes a fourfold decrease compared with undeformed crystals (Table I). The exciton gas density n_{ex} increases then by approximately one order of magnitude, making the conditions favorable for the observation of the biexciton. The concentration n_M of biexcitons that are in thermodynamic equilibrium with the exciton gas can be estimated from the formula[17]

$$n_M = n_{ex}^2 (4\pi\hbar^2/kTm_{ex})^{3/2} g_M/g_{ex}^2 \exp(\Delta/kT), \tag{5}$$

where g_M is the statistical weight of the biexcitons and Δ is the binding energy of the biexciton. From estimates of n_M according to (5) in which the experimental values of n_{ex} and $\Delta = 0.4$ meV[18] are substituted it follows that for Si (1-2) the partial pressures of the excitons and biexcitons are of the same order along

the liquid–gas coexistence lines, whereas in Si (2–6) we have the ratio $n_M/n_{ex} \leqslant 10^{-2}$.

We have previously reported observation of RR of biexcitons in Si (1–2) under pulsed excitation.[19] The kinetics of the RR spectra of Si (1–2) ($p \sim 25$ kgf/mm^2) under pulsed excitation of 30 kW/cm^2 and at $T = 1.8$ K are shown in Fig. 2. At the instant of the pulse, the EHL radiation (L band) predominates. The spectra show clearly the emission line FE of the free excitons, but there are not lines of exciton-impurity complexes. In addition to the L and FE lines, the spectra contain also one M line that appears at deformations $p \geqslant 20$ kgf/mm^2. The distance between the maxima of the lines M and FE does not depend on the pressure and equals 2 meV. After the damping of the EHL emission band, the shape of the "red" wing of the M line remains unchanged, and the damping time of the M line is τ_M $\sim 0.6\tau_{ex}$ (Fig. 3). The M line was observed in the RR spectrum up to 10 K.

We attribute the M line in the Si (1–2) spectrum to the biexciton-recombination mechanism in accord with the conservation law

$$E_K^{II} = E_k^I + \hbar\Omega^{TO} + \hbar\omega, \qquad (6)$$

where E_K^{II} and E_k^I are the energies of the biexciton and exciton, respectively. The biexciton origin of the M line is confirmed by experiments performed under conditions of stationary volume excitation. Figure 4 shows the evolution of the recombination spectrum of Si (1–2) at $p = 50$ kgf/mm^2 in the region of the exciton structure under stationary laser excitation ($\lambda = 1.064$ μm) and at $T = 1.8$ K. With the aid of such a source it is possible to obtain volume excitation in Si (1–2) crystals starting with a deformation $p \geqslant 20$ kgf/mm^2. The spectra corresponds to measurements of the average exciton concentration in the interval $10^{14} - 8 \cdot 10^{14}$ cm^{-3}. At minimum pumps the spectrum reveals the exciton emission and the RR line BE of an exciton bound to a neutral acceptor. With increasing excitation density, the intensity of the BE line remains practically unchanged. An M line appears then between the BE and
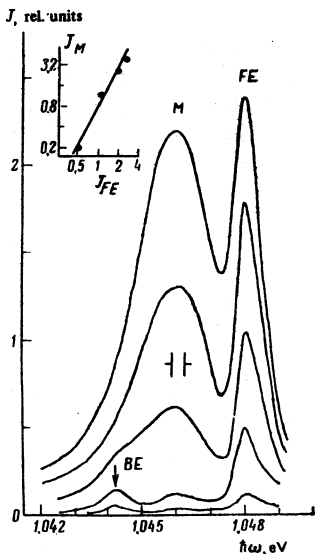
FE lines, and its intensity increases in the indicated range of exciton concentrations in proportion to the square of the exciton-line intensity (insert of Fig. 4). This is one of the confirmation of the molecular origin of the M band.

At concentrations $\bar{n} > 10^{15}$ cm^{-3} and $T = 1.8$ K the intensity ratio of the lines FE and M ceases to depend on the pump. It is illustrated in Fig. 5, which shows three spectra obtained at different deformations and at the maximum quasistationary pump attained in our experiments (~ 5 kW/cm^2). With increasing pressure, the RR spectra shift in the red direction and the absorption coefficient in the exciting-wavelength region increases, and with it the average concentration of the excited e–h pairs, while the ratio J_M/J_{ex} remains constant at $p > 50$ kgf/mm^2 and is approximately equal to the ratio J_M/J_{ex} under pulsed excitation. This behavior can be understood if it is assumed that at $T \sim 1.8$ K the condensation in the EHL begins at $n_{ex} \sim 10^{15}$ cm^{-3}. Thus, experiments with quasistationary volume excitation of Si (1 – 2) also show that the partial pressures of the excitons and biexcitons in the gas phase are of the same order at densities $\bar{n}$ at which condensation into EHL sets in.

6. CALCULATION OF THE BIEXCITON ANNIHILATION AMPLITUDE

In the considered case of indirect electronic transitions, the annihilation of a biexciton results into production of a photon, phonon, and exciton. The corresponding line in the luminescence has a finite width even if the biexciton is initially at rest; this width is due to the fraction of its energy that the biexciton gives up to the remaining exciton.

Assume that in the initial state we have a biexciton with quasimomentum $2\mathbf{k}_0 + \mathbf{P}$, made up of two electrons (1 and 2) near the minimum of the conduction band, with quasimomenta $\mathbf{k}_0 + \mathbf{k}_1$ and $\mathbf{k}_0 + \mathbf{k}_2$, and two holes ($a$ and b) in the valence band with quasimomenta $\mathbf{k}_a$ and $\mathbf{k}_b$. In the second-quantization representation, the corresponding state is given by

$$|\mathbf{P}\rangle = \sum_{\mathbf{k}} C^P(\mathbf{k}_1\mathbf{k}_2|\mathbf{k}_a\mathbf{k}_b)\chi(\sigma_1\sigma_2|\sigma_a\sigma_b)$$

$$\times a^+(\mathbf{k}_0+\mathbf{k}_1,\sigma_1)a^+(\mathbf{k}_0+\mathbf{k}_2,\sigma_2)b^+(\mathbf{k}_a,\sigma_a)b^+(\mathbf{k}_b,\sigma_b)|\Phi_0\rangle,$$

where χ is the spin wave function, σ is the spin projection, a^+ and b^+ are the electron and hole creation operators, and C^P is the Fourier transform of the coor-
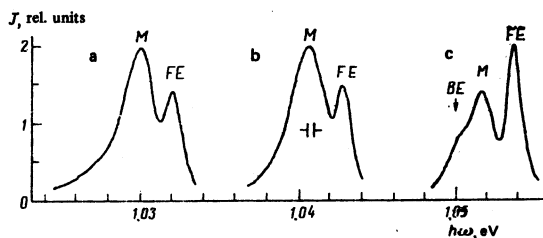
J, rel. units

FIG. 4. Variation of RR of Si (1–2) ($p \sim 45$ kgf/mm^2; $T = 1.8$ K) with changing excitation density as $\bar{n}$ is increased from $\sim 10^{14}$ to $\sim 10^{15}$ cm^{-3}. The insert shows the $J_M(J_{FE})$ dependence in a logarithmic scale, and the straight line corresponds to $J_M - J_{FE}^2$.

J, rel. units

FIG. 5. Change of RR spectra of Si (1–2) excited by a laser with $\lambda = 1.064$ μm (~ 500 W/cm^2) with increasing uniaxial deformation: a—60 kgf/mm^2, b—50 kgf/mm^2, c—40 kgf/mm^2.

dinate wave function of the biexciton in the effective-mass (EM) method:

$$C^P(k_1 k_2 | k_a k_b) = \int dr_1\, dr_2\, dr_a\, dr_b\, \Psi^P(r_1 r_2 | r_a r_b) \exp\{-i(k_1 r_1 + k_2 r_2 + k_a r_a + k_b r_b)\}.$$

An analogous expression can be written for the final state—an exciton with quasimomentum $k_0 + Q$ and a phonon with quasimomentum $k_0 + q$:

$$|Q, q\rangle = \sum C^Q(k_e | k_h) \chi(\sigma_e | \sigma_h) d^+(k_0 + q) a^+(k_0 + k_e, \sigma_e) b^+(k_h, \sigma_h) |\Phi_0\rangle,$$

where C^Q is connected with the wave function of the exciton

$$C^Q(k_e | k_h) = \int dr_e\, dr_h\, \Psi^Q(r_e | r_h) \exp\{-i(k_e r_e + k_h r_h)\},$$

and d^+ is the phonon creation operator.

The matrix element of the transition is obtained in standard fashion in second-order perturbation theory (interaction with the phonons and the electromagnetic field), and reduces after simple transformations to the form

$$M(P | q, Q) \sim \int dr\, dr_e\, dr_h\, \Psi^P(r, r_e | r, r_h) e^{-iqr} \Psi^{*Q}(r_e | r_h). \qquad (7)$$

In the derivation it was assumed that the spin function of the electrons and holes in the biexciton is antisymmetrical with respect to permutation of two electrons or two holes, while the coordinate function is symmetrical.

Formula (7) is a generalization of the well-known Elliott–Sakharov formula[20,21] for the exciton-annihilation amplitude, which is proportional to $\Psi_{ex}(0)$, and admits also of a simple physical interpretation. In fact, it is seen from (7) that this is the probability amplitude of finding in the biexciton one of the electrons and one of the holes in one place, while the other electron and hole form an exciton with a wave function Ψ^Q.

It follows from the translational invariance of the exciton and biexciton, in the EM method, that $M(P | q, Q)$ contains $\delta(P - q - Q)$, i.e., the quasimomentum conservation law holds. In addition, it is easy to verify that by virtue of the independence of the internal motions in the exciton and the biexciton of the motion of the gravity center, the function $M(P | q, Q)$ after separating the δ function will depend only on one linear combination of the remaining two independent vectors

$$M(P | q, Q) = \delta(P - q - Q) N(2Q - P). \qquad (8)$$

To determine M explicitly we must know the wave function of the ground state of the biexciton. There is no exact solution of this problem, and we use therefore the best of the known variational approximations.[18] For the case of equal isotropic masses of the electrons and holes, it was found in[16] that

$$\Psi^P = \exp\{iP(r_1 + r_2 + r_a + r_b)/A\} \psi F / S, \qquad (9)$$

where

$$\psi = 2 \exp\{-k(r_{1a} + r_{2a} + r_{1b} + r_{2b})/2a_B\} \cos\{k\beta(r_{1a} + r_{2b} - r_{1b} - r_{2a})/2a_B\},$$

$$S^2(r_{ab}) = \int dr_1\, dr_2\, \psi^2,$$

$$F(r_{ab}) = (r_{ab}/Aa_B) \exp(-r_{ab}/Aa_B) + C \exp(-r_{ab}B/Aa_B),$$

$$k = 1.18, \quad \beta = 0.66, \quad A = 1.14, \quad B = 0.36, \quad C = 0.39$$

$a_B = 2\varkappa \hbar^2/m^* e^2$ is the Bohr exciton radius, $r_{1a} = |r_1 - r_a|$, etc. After substituting in (7) the expression (9) for the biexciton wave function, and also the expression

$$\Psi^Q(r_e | r_h) = \exp\{iQ(r_e + r_h)/2 - r_{eh}/a_B\}$$

for the wave function of the exciton, and after numerical integration, we obtain the function N. The values of $N(K)$ for $Ka_B \leq 2.5$, accurate to a constant factor, are listed in Table II, from which it can be seen, in particular, that almost the entire function N is concentrated in the region $Ka_B \leq 2$.

7. BIEXCITON LINE SHAPE

If we neglect the dispersion of the phonon (in our case, a TO phonon), then we can obtain for the probability of emission of light frequency ω the expression

$$\begin{aligned} W(\hbar\omega) \sim \int dP\, dQ \exp(-P^2/8m^*kT) \\ \times N^2(|2Q - P|) \delta(E_P^{II} - E_Q^I - \hbar\omega - \hbar\Omega), \end{aligned} \qquad (10)$$

where E_P^{II} is the biexciton energy, E_Q^I is the exciton energy, and $\hbar\Omega$ is the phonon energy.

At sufficiently low temperatures, such that the average thermal momentum $\langle P \rangle$ of the biexciton satisfies the inequality $\langle P \rangle a_B \ll 1$, we can see from (10) that the line shape is given by the expression

$$W(\hbar\omega) \sim |Q| N^2(2Q) \qquad (11)$$

at

$$Q^2/4m^* = E_0^I - \hbar\Omega - \Delta - \hbar\omega,$$

where $\Delta = 2E_0^I - E_0^{II}$ is the biexciton binding energy. Figure 6 shows the experimental luminescence line at the temperature $T \sim 1.8$ K together with the theoretical relation (11), the function N being taken from Table II. The following was assumed: the binding energy of the exciton is 12 meV,[22] $a_B = 52.5$ Å, and the binding energy Δ corresponding to the trial function (9) is equal to 0.4 meV. The agreement between theory and experiment seems quite satisfactory to us.

We note that the biexciton binding energy estimate used in[19,23] and based on fitting the experimental

TABLE II. The function $N(a_B P)$.

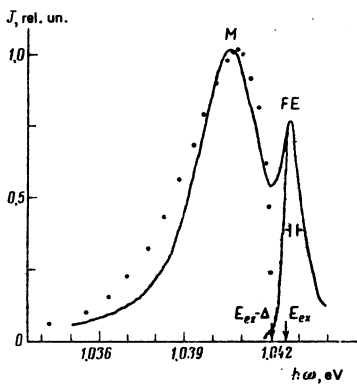| $a_B P$	$N(a_B P)$	$a_B P$	$N(a_B P)$	$a_B P$	$N(a_B P)$
0.1	4.87	0.9	3.14	1.6	0.96
0.2	4.79	1.0	2.81	1.7	0.73
0.3	4.67	1.1	2.47	1.8	0.52
0.4	4.50	1.2	2.14	1.9	0.34
0.5	4.28	1.3	1.82	2.0	0.20
0.6	4.04	1.4	1.51	2.5	−0.12
0.7	3.76	1.5	1.23	3.0	−0.01
0.8	3.46				

FIG. 6. Comparison of the calculated RR spectrum of a biexciton (points) with the experimental one. The figure shows also the RR spectrum of the exciton (FE) obtained at low excitation density. $T = 1.8$ K.

[4]V. S. Bagaev, T. I. Galkina, O. V. Gogolin, and L. V. Keldysh, Pis'ma Zh. Eksp. Teor. Fiz. **10**, 309 (1969) [JETP Lett. **10**, 195 (1969)].

[5]B. M. Ashkinadze, I. P. Kretsu, A. A. Patkin, and I. D. Yaroshetskiĭ, Fiz. Tekh. Poluprovodn. **4**, 2206 (1970) [Sov. Phys. Semicond. **4**, 1897 (1971)].

[6]J. A. Thomas, T. M. Rice, and J. C. Hensel, Phys. Rev. Lett. **33**, 219 (1974).

[7]R. B. Hammond, T. C. McGill, and J. W. Mayer, Phys. Rev. B **13**, 3566 (1976).

[8]R. B. Hammond, D. L. Smith, T. C. McGill, Phys. Rev. Lett. **35**, 1535 (1975).

[9]A. A. Abrikosov, L. P. Gor'kov, and I. E. Dzyaloshinskiĭ, Metody kvantovoĭ teorii polya v statisticheskoĭ fizike (Quantum Field Theoretical Methods in Statistical Physics), Fizmatgiz, 1962 [Pergamon, 1965].

[10]P. T. Landsberg, Phys. Status Solidi B **15**, 623 (1966).

[11]H. L. Störmer, R. W. Martin, and J. C. Hensel, Proc. Thirteenth Intern. Conf. on Physics of Semiconductors, Rome, 1976.

[12]P. Vashishta, J. P. Bhattacharyya, and K. S. Singwi, Phys. Rev. B **10**, 5108 (1974).

[13]P. Vashishta, S. G. Das, and K. S. Singwi, Phys. Rev. Lett. **33**, 911 (1974).

[14]R. N. Silver, Phys. Rev. B **12**, 5689 (1975).

[15]S. G. Tikhodeev, Kratk. Soobshch. Fiz. **5**, 13 (1975).

[16]V. S. Bagaev, N. V. Zamkovets, L. V. Keldysh, N. N. Sibel'din, and V. A. Tsvetkov, Zh. Eksp. Teor. Fiz. **70**, 1501 (1976) [Sov. Phys. JETP **43**, 783 (1976)].

[17]Z. A. Insenov, G. E. Norman, and L. Yu. Shurova, Zh. Eksp. Teor. Fiz. **71**, 1960 (1976) [Sov. Phys. JETP **44**, 1028 (1976)].

[18]W. F. Brinkman, T. M. Rice, and B. Bell, Phys. Rev. B **8**, 1570 (1973).

[19]V. D. Kulakovskiĭ and V. B. Timofeev, Pis'ma Zh. Eksp. Teor. Fiz. **25**, 487 (1977) [JETP Lett. **25**, 458 (1977)].

[20]R. J. Elliott, Phys. Rev. **108**, 1384 (1957).

[21]A. D. Sakharov, Zh. Eksp. Teor. Fiz. **18**, 631 (1948).

[22]G. L. Bir and G. B. Pikus, Simmetriya i deformatsionnye éffekty v poluprovodnikakh (Symmetry and Deformation Effects in Semiconductors), Nauka, 1972.

[23]I. Pelant, A. Mysyrowicz, and C. Benoit à la Guillaume, Phys. Rev. Lett. **37**, 1708 (1976).

contour with the aid of a model-derived expression for the matrix element $M(\mathbf{P}|\mathbf{q}, \mathbf{Q})$, is logically contradictory. In fact, as seen from (7), both the line shape and the binding energy are uniquely determined by the wave function of the biexciton and are consequently not independent quantities. Thus, on the basis of the analysis of the shape it is impossible to determine exactly the true value of the biexciton binding energy.

Assuming thermodynamic equilibrium in the gas phase, the biexciton binding energy was estimated by us from the temperature dependence of the ratio of the exciton and biexciton line intensities in the interval $T = 2$ to 4.2 K and turned out to be $\Delta = 0.55 \pm 0.15$ meV.

[1])Secs. 2 and 5 were written by two of the authors (V. K. and V. T.), Sec. 6 by the third (V. E.), and Sec. 7 by all three of us.

[1]Ya. E. Pokrovskiĭ, Phys. Status Solidi A **11**, 385 (1972).

[2]J. D. Jeffries, Science **189**, 955 (1975).

[3]A. F. Dite, V. D. Kulakovskiĭ, and V. B. Timofeev, Zh. Eksp.

Translated by J. G. Adashko

Critical magnetic fields of molybdenum chalcogenides

N. E. Alekseevskiĭ, A. V. Mitin, C. Bazan,[1] N. M. Dobrovol'skiĭ, and B. Raczka[1]

Institute of Physical Problems, Academy of Sciences, USSR
(Submitted 18 August 1977)
Zh. Eksp. Teor. Fiz. **74**, 384–388 (January 1978)

The critical temperatures T_c and upper critical magnetic fields $H_{c2}(T)$ have been measured for a number of molybdenum sulfides prepared from Mo_6S_8Pb and Mo_6S_8Sn. It is shown that introduction of additional components into these compounds can lead to a simultaneous increase of T_c and $H_{c2}(0)$. The maximum critical field $H_{c2}(0) = 0.58$ MOe is observed in a specimen of the composition $Mo_6S_8PbGa_{0.4}W_{0.4}$, for which $T_c = 14.9$ K.

PACS numbers: 74.70.Dg, 74.70.Lp

Among the superconductors within the last decade, great interest attaches to systems in which the superconductivity is retained in superhigh magnetic fields. Such systems include, for example, molybdenum sulfide to which has been added a small amount of lead.

Thus the compound of composition $Mo_{5.1}S_6Pb$ has a critical field $H_{c2}(0)$ exceeding 0.5 MOe.[1] It seemed of interest to conduct investigations of the upper critical fields H_{c2} of several new molybdenum chalcogenides, and also to repeat the measurements of such systems